THE ASTROPHYSICAL JOURNAL, 338:417–423, 1989 March 1

STUDIES OF HOT B SUBDWARFS. VII. NON–LTE RADIATIVE ACCELERATION OF HELIUM IN THE ATMOSPHERES OF sdOB STARS

G. MICHAUD,[1,2] P. BERGERON,[2] U. HEBER,[3] AND F. WESEMAEL[2]

Received 1988 April 28; accepted 1988 August 10

ABSTRACT

Detailed non–LTE radiative accelerations on He are calculated in non–LTE model atmospheres with parameters appropriate for sdOB stars. Detailed statistical equilibrium calculations are carried out in order to obtain helium occupation numbers.

For $N(\mathrm{He})/N(\mathrm{H}) = 0.1$, the radiative accelerations are calculated to be always at least 10 times smaller than gravity in the line-forming region, so that He should always be underabundant, as observed in these objects. However, the radiative acceleration remains smaller than gravity even at the observed underabundances of He so that, in the absence of competing processes, diffusion should lead to larger underabundances than observed. The observed He abundances in sdOB stars cannot be supported by radiative acceleration alone. Other processes, such as mass loss, must be involved.

Calculations are also carried out with different levels of approximation. It appears that, for many purposes, radiative accelerations calculated in LTE models but with a non–LTE ionization balance may be sufficient. It is also shown that, for He, a formula based on the diffusion approximation to the radiative flux gives estimates of the radiative acceleration accurate to within a factor of 3.

Subject headings: radiative transfer — stars: abundances — stars: atmospheres — stars: early-type — stars: subdwarfs

I. ASTROPHYSICAL CONTEXT

The class of subluminous hydrogen-rich stars includes the classical subdwarf B stars (sdBs), discussed in Greenstein and Sargent (1974), and the hotter ($T_{\mathrm{eff}} \geq 35{,}000$ K) sdOB stars, first introduced by Baschek and Norris (1975). Stars in both subgroups are characterized by helium-deficient atmospheres; recent analyses of two dozens sdB and sdOB stars have revealed helium number fractions well below 0.06 (Hunger *et al.* 1981; Baschek, Höflich, and Scholz 1982; Baschek *et al.* 1982; Heber *et al.* 1984*a*, *b*; Heber 1986). Although there seems to be a mean trend for the He abundance to increase with T_{eff}, the scatter of individual abundances, especially for the sdOBs, is very large (Heber 1986). Helium abundances were found to differ by one order of magnitude at the same atmospheric parameters (T_{eff} and gravity). Therefore, a correlation between He abundance and atmospheric parameters among the H-rich subdwarfs cannot be established. In addition, abundance anomalies of many elements, most strikingly C and Si, have been reported in several sdOB stars (Baschek, Höflich, and Scholz 1982; Baschek *et al.* 1982; Heber *et al.* 1984*a*; Lynas-Gray *et al.* 1984; Lamontagne *et al.* 1985; Lamontagne, Wesemael, and Fontaine 1987). Diffusion processes, possibly in the presence of competing mechanisms such as mass loss, are the likely source of these abundance anomalies.

Evidence has accumulated (Heber *et al.* 1984*b*; Heber 1986) showing that the sdB and sdOB stars can be identified with evolutionary models for the so-called extended horizontal branch (EHB). These models represent the blue end of the horizontal branch and, therefore, have a very low envelope mass ($<0.02\ M_{\odot}$). Their internal structure differs from the conventional horizontal branch models, because the hydrogen-rich envelope is inert (i.e., the luminosity of the hydrogen burning shell is negligibly small). In this respect EHB models bear great resemblance to helium main-sequence models to which a thin hydrogen-rich envelope is added. The analysis of their abundance patterns can be used to obtain an independent check on the validity of the EHB interpretation. In particular, the evolutionary time scale might be constrained by the observed abundance anomalies (Michaud *et al.* 1985). Moreover, the latter become probes into the hydrodynamics that govern the external regions of the hydrogen-rich subdwarfs. In particular, the mass-loss rate has been shown to be closely related to the observed underabundance of Si (Michaud *et al.* 1985). It could also be constrained by the He abundance (Heber 1986). Using the observed He abundance to constrain hydrodynamic properties requires that the terms entering the diffusion equations be well determined. In particular, the radiative acceleration must be known to a factor of about 1.3 (Michaud 1987) to allow precise determinations of abundances in the presence of mass loss. Unfortunately, the current estimates of radiative accelerations for He (Michaud *et al.* 1979; Vennes 1985) are accurate only in stellar interiors since they were obtained with the diffusion approximation to the radiative transfer. Such calculations cannot, *a priori*, be claimed to be appropriate for stellar atmospheres.

Our aim in this paper is to calculate the radiative acceleration of He with as much accuracy as possible using complete non–LTE models that include detailed atomic models of He and H. This non–LTE radiative acceleration will be compared to more approximate calculations to give a measure of the inaccuracies involved in the various approximations. This should help decide under which circumstances detailed non–LTE calculations are needed for estimates of radiative accelerations.

The calculations of the radiative accelerations are described in § II, while the results are presented in § III. In § IV, a brief

[1] Killam Foundation Fellow.
[2] Département de physique, Université de Montréal.
[3] Institut für Theoretische Physik und Sternwarte der Universität Kiel.

comparison to observations will be made along with a discussion of the degree of accuracy required to obtain reliable radiative accelerations.

II. CALCULATIONS

a) The Non–LTE Model Atmospheres

The non–LTE model atmospheres used here are described in the detailed analysis of Feige 110 by Heber *et al.* (1984*a*). Statistical equilibrium calculations for helium were carried out using a He model atom with 62 levels: respectively 15 and 14 levels for the singlet and triplet systems of He I, 32 levels for He II, and the He III continuum. The He III continuum and all 29 levels of He I were allowed to depart from LTE. For He II, only the 10 lowest were in non–LTE, the other levels being in LTE with He III.

Model atmospheres were calculated with different gravities ($5 \le \log g \le 6$), effective temperatures ($40{,}000 \le T_{\rm eff} \le 60{,}000$ K), and helium-to-hydrogen ratios ($0.0002 \le N(\mathrm{He})/N(\mathrm{H}) < 0.1$), in order to cover the range of parameters appropriate for sdB and sdOB stars. The atmospheric parameters selected thus include those determined for Feige 110 in the analysis of Heber *et al.* (1984*a*; $T_{\rm eff} = 40{,}000$ K, $\log g = 5.0$, $N(\mathrm{He})/N(\mathrm{H}) = 0.03$) and the hydrogen-rich subdwarf LB 3459 (Kudritzki *et al.* 1982). Not only are these stars particularly well-studied but their $T_{\rm eff}$ are often mentioned as the lower limit of the He rich sdO stars (e.g., Groth, Kudritzki, and Heber 1985). It is especially important to calculate the radiative acceleration near that $T_{\rm eff}$ to check if radiative acceleration may not play a role in causing the He-rich phenomenon.

b) The Radiative Acceleration Calculations

When an element absorbs a photon, part of the momentum is transferred to the atom. We distinguish between line absorption, where a photon excites one electron from one level to another, and continuous absorption, where a photon ionizes an atom. In the first process, all the momentum of the incoming photon is transferred to the atom. In continuous absorption, only part of the momentum is transferred to the atom since the electron carries away some linear momentum. Continuous absorption is negligible for heavy elements (Michaud *et al.* 1976), but not for helium (Michaud *et al.* 1979). We have thus taken into account both processes in our calculations.

The radiative acceleration transferred to the lines of, for example, He I is given by

$$F_{\mathrm{L\,I}} = \frac{4\pi}{c}\frac{1}{X(\mathrm{He\ I})}\int_0^\infty K_\nu(\mathrm{He\ I})H_\nu\,d\nu\,, \tag{1}$$

where H_ν is the Eddington monochromatic flux, X(He I) is the mass fraction of He I, and K_ν(He I) is the monochromatic opacity of the lines of He I given by

$$K_\nu(\mathrm{He\ I}) = \frac{1}{\rho}\sum_i\sum_{j>i}\left[n_i - \frac{g_i n_j}{g_j}\right]\alpha_{\nu ij}\,. \tag{2}$$

Note that we use K_ν, the opacity per unit volume and *not* per unit mass as, for instance, Mihalas (1978) does. Our equation (2) is equivalent to his equation (4–13). The n_i and g_i are the level density and statistical weight, respectively; the indices i and j refer to the lower and upper level, respectively.

In equation (2), the summations must be taken over all excited levels available to the ion. The non–LTE populations are directly fed from the input model. The $\alpha_{\nu ij}$ are the line absorption cross sections; for He I lines, these have been evaluated using a Voigt profile with the electronic pressure widths and ionic corrections of Bassalo, Cattani, and Walder (1982) and Dimitrijevic and Sahal-Bréchot (1984). For the He II cross sections, we used the formalism of Griem (1960). The satistical weights and oscillator strengths were taken from Wiese, Smith, and Glennon (1966). The last level available for each ion has been calculated using a modified version of the Debye screening formalism.

In equation (1), each ionization state must be considered separately. Following the discussion of Martel (1979), eight lines of He I and 13 lines of He II have been retained for the radiative acceleration calculations. These are the most important lines in terms of radiative support (see § III). The frequency integration in equation (1) is carried out for each line and extends out to the point where the line opacity reaches 10^{-5} the continuous opacity.

The radiative acceleration produced by each of the helium continua can be calculated in similar fashion. Equation (1) is now replaced by

$$F_{\mathrm{C\,II}} = \frac{4\pi}{c}\frac{1}{X(\mathrm{He\ II})}\int_{\nu_0}^\infty K_{\nu C}(\mathrm{He\ I})H_\nu\left[1.6\frac{\nu_0}{\nu} - 0.6\right]d\nu\,, \tag{3}$$

where ν_0 is the threshold frequency of ionization of He I. Note that, because of ionization, the momentum of a photon that ionizes He I is in fact given to He II and so the radiative acceleration is labeled $F_{\mathrm{C\,II}}$. Similarly, the radiative acceleration transferred through the continuum of He II is labeled $F_{\mathrm{C\,III}}$. The term in square brackets is the correction for the fraction of the momentum given to the electron in the ionization (see Michaud 1970), as obtained by Sommerfeld (1939) for the H ground state. To our knowledge, this is the only case that has been calculated so far and this correction will be used here for all levels of He I and He II. This correction reduces the radiative acceleration transferred through the He I and He II continua by a factor of order 2. It will be further discussed in § IV. The continuous monochromatic opacity $K_{\nu C}$(He I) was calculated in non–LTE:

$$K_{\nu C}(\mathrm{He\ I}) = \frac{1}{\rho}\sum_i\left[n_i - n_i^*\exp\left(-\frac{h\nu}{kT}\right)\right]\alpha_{\nu iC}\,, \tag{4}$$

where n_i^* denotes the LTE population. The continuum cross sections $\alpha_{\nu iC}$ were calculated using subroutines from the ATLAS program (Kurucz 1970).

Finally, the Eddington fluxes were calculated by solving the radiative transfer equation with the Feautrier method. In doing so, we made use of the non–LTE source function:

$$S_\nu = \frac{n}{K_\nu}\,, \tag{5}$$

where K_ν is the total opacity including hydrogen and helium lines, hydrogen and helium continua, free-free processes, and electron scattering. The non–LTE emissivity n is given by

$$n = \frac{2h\nu^3}{\rho c^2}\left[\sum_i\sum_{j>i}\frac{g_i}{g_j}n_j\alpha_{\nu ij} + \sum_i n_i^*\alpha_{\nu iC}\exp\left(-\frac{h\nu}{kT}\right) + \sum_C n_e n_C\alpha_{\nu CC}(T)\exp\left(-\frac{h\nu}{kT}\right)\right]. \tag{6}$$

In equation (6), $\alpha_{\nu CC}$ is the cross section of the free-free process for the state of ionization and element represented by

C and n_C is the number density. Those of H II, He II, and He III were included.

Once the individual contribution of each process to the radiative acceleration has been calculated, some care must be taken in averaging them. We have followed here the procedure outlined by Montmerle and Michaud (1976; see, in particular, their eqs. [6.11] and [6.16]), together with the latest diffusion coefficients of Paquette *et al.* (1986). The random walk of electrons in the singlet states of He I and in He II was solved as described in Michaud *et al.* (1979). Once these redistribution and averaging processes have been taken into account, we obtain the effective radiative acceleration transferred through each process (line or continuum) of each state of ionization. These terms are labeled in the following figures He I_L, He II_L, He II_C, and He III_C.

c) *Some Additional Heuristic Calculations*

In order to determine the size of the non–LTE effects, calculations were also carried out in LTE model atmospheres with different approximations to the non–LTE populations.

Despite the increasing availability of non–LTE models, less sophisticated methods to evaluate radiative forces in subdwarf atmospheres are often used to obtain first estimates; they are also useful for elements for which non–LTE calculations are impractical to carry out. For example, LTE radiative forces have been estimated recently in an investigation of the radiative support of heavy elements in hot subdwarf stars (Michaud *et al.* 1985; Bergeron *et al.* 1988). What are the changes brought about if a similar approximation is used to evaluate the radiative support of helium? How reliable are LTE estimates?

With these considerations in mind, we have carried out two additional sets of radiative acceleration calculations. The first set consists of LTE radiative accelerations calculated using a grid of LTE model atmospheres similar to those of Wesemael *et al.* (1980). In a second set of calculations, the basic stratification of the LTE models is again used; however, the LTE atomic populations entering into the calculations of g_R are now calculated with the Saha-Boltzmann equation at a radiation temperature rather than at the usual thermodynamic temperature (see, e.g., Mihalas 1978, p. 123ff). This radiation temperature is defined as the temperature of the radiation field at the frequency of the ionization threshold. It will be shown below that, as we had anticipated, this hybrid approach incorporates the dominant non–LTE effect on the calculation of radiative accelerations, namely the nonlocal nature of the photon flux in the optically thin layers. Further information on this approach are found in Bergeron *et al.* (1988).

III. RESULTS

a) *Non–LTE calculations of g_R*

The main results of the non–LTE radiative acceleration calculations are shown in Figure 1. On panels *a* and *b* are shown the contribution of each process (*dashed curves*) to the total radiative acceleration in models with T_{eff} = 40,000 and 60,000 K respectively (N(He)/N(H) = 0.03, log g = 5.0). The full line is the total radiative acceleration. The contribution of the lines of He I is indicated by He I_L, that of the continuum of He I by He II_C (see eq. [3]), and so on. The total radiative acceleration should be compared to the almost horizontal dashed line which shows the gravity of the model corrected for the effect of the local electric field (Montmerle and Michaud 1976). In what follows this effective gravity is referred to as gravity. Thermal diffusion has been neglected since Paquette *et al.* (1986) have shown that its effect was typically a factor of 2 smaller than calculated by Michaud *et al.* (1979) who had used the asymptotic low-density approximation of Chapman and Cowling (1970). If included, it would increase the effective gravity by some 20% or less. The approximate line-forming region (τ_{5000} = 0.1) is indicated by a vertical line on the lower scale.

At T_{eff} = 40,000 K, the largest contribution to the radiative acceleration in the line-forming region is due to the continuum of He I, labeled He II_C, followed by the contribution of the He II lines (He II_L) and continuum (He III_C). The lines of He I contribute substantially but their contribution does not dominate. This is contrary to the results of Michaud *et al.* (1979) where, in their Figure 1, the maximum at T_4 = 3 is due to the contribution of the lines of He I. This behavior is explained in § III*c*.

It is important to verify that enough lines of He have been included in the calculations. We discuss the case of He II since its lines end up being more important than those of He I. The lines normally included are the first three from the fundamental of He II and the first 10 from the first excited state. We first verified the effect of adding 10 lines from two higher up levels. We added five lines from level n = 3 and five from level n = 4. The contribution of the lines of He II to the radiative acceleration is increased everywhere by less than 30%. Below the line-forming region, adding lines from the fundamental could have increased the contribution of the lines of He II significantly. Each new line added contributes a fraction of 0.66 that of the preceding line. It is easy to verify that the inclusion of an infinite number of terms of that series would multiply the contribution of the first three terms of the series by a factor of 1.4. However, the lines of He II contribute only 10% of the total He radiative acceleration there, so that an increase by a factor of 1.4 of the radiative acceleration through the lines causes only a 4% increase of the total g_R.

At T_{eff} = 60,000 K (panel *b*), the main contribution always comes from the continuum of He II, labeled He III_C, with a major contribution of the lines of He II. At this T_{eff} there is not enough He I for its contribution to be substantial, in contrast to the situation at T_{eff} = 40,000 K.

b) *Abundance, Gravity, and T_{eff} Effects*

As expected, reducing the He abundance increases the radiative acceleration (see panel *c*; T_{eff} = 40,000 K, log g = 5). When N(He)/N(H) = 0.1, the radiative acceleration in the line-forming region is about 1/30 of gravity and it is about 3 times larger (0.1 gravity) if the abundance is reduced by a factor of 10. This is expected, since the reduction of the abundance decreases saturation, and so increases the photon flux and the radiative acceleration. The radiative acceleration should be able to support an apparent abundance of about 0.0002 to 0.001. For such an abundance, the radiative acceleration is still smaller than gravity at τ_{5000} = 0.1, the approximate line-forming region. The radiative acceleration increases with depth, however, and becomes larger than gravity for $\tau_{5000} > 1$. The lines would appear broad since the line-forming region would be located deeper than usual. A comparison of the contribution of the different processes as a function of abundance (not shown) reveals that modifying the abundance changes the relative contribution of the lines and of the continuum: these do not react in the same way to a change of abundance. The difference is never very large, however.

On panel *d* are shown similar results in a model with log g = 6. The gravity change is partly compensated by a lower

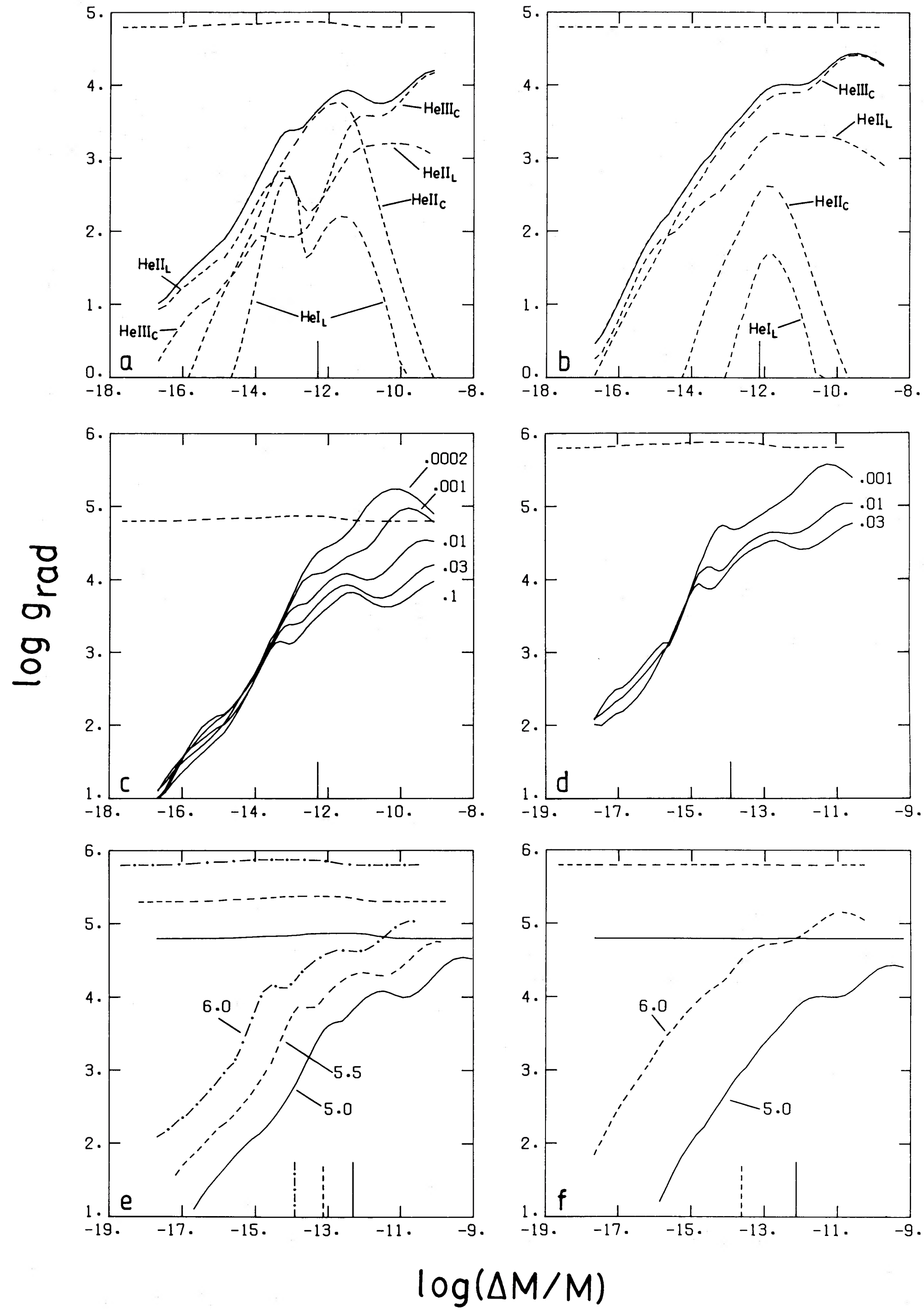

FIG. 1.—Radiative acceleration on He as a function of mass fraction above the point of interest. Panels *a* and *b* are for models at log $g = 5$, $N(\mathrm{He})/N(\mathrm{H}) = 0.03$, with $T_{\mathrm{eff}} = 40{,}000$ and 60,000 K, respectively. The solid curve is the total radiative acceleration, while the other curves are the contribution of the various processes. The contribution of the lines of He I is identified by He I$_L$ and that of the continuum of He I by He II$_C$ (and so on). On each panel, the nearly horizontal dashed line indicates effective gravity (see text), while the approximate line-forming region ($\tau_{5000} = 0.1$) is indicated by vertical line on the lower scale. Panels *c* and *d* show the total radiative acceleration for models at $T_{\mathrm{eff}} = 40{,}000$ K, log $g = 5.0$ and 6.0, respectively. Each curve is labeled by the He number fraction. Panels *e* and *f* show the total radiative acceleration for models at $T_{\mathrm{eff}} = 40{,}000$ K, $N(\mathrm{He})/N(\mathrm{H}) = 0.01$ and $T_{\mathrm{eff}} = 60{,}000$ K, $N(\mathrm{He})/N(\mathrm{H}) = 0.03$, respectively. Each curve is labeled by the surface gravity. More than one model is shown on each figure and the line-forming region is shown for each by an appropriate vertical line.

ionization, leading to an increase in the radiative acceleration, so that the ratio of gravity to radiative acceleration is not strongly modified. It however goes up slightly as gravity increases, as is better seen from panel *e* of the figure for $N(\mathrm{He})/N(\mathrm{H}) = 0.01$. Similar remarks apply at $T_{\mathrm{eff}} = 60{,}000$ K (panel *f*), where gravity effects are also shown.

A comparison between the 40,000 K and 60,000 K models ($\log g = 5.0$, $n(\mathrm{He})/N(\mathrm{H}) = 0.03$) of panels *c* and *f* shows that a 20,000 K increase in T_{eff} increases the radiative acceleration by a factor of about 2 in the line-forming region. A comparison with calculations in a model with $T_{\mathrm{eff}} = 45{,}000$ K (not shown) shows that a 5000 K increase in the T_{eff} leads to an increase of only 1.3 in the radiative acceleration, while the luminosity is increased by a factor of 1.6. This small variation of g_R with T_{eff} (or L) can be understood in terms of an increased ionization which reduces the fraction of the flux absorbed by He.

c) Contribution of the He I *Lines*

Since the mean free path of He I is much larger than that of He II, it is important to determine whether, after the line absorption of a photon, He I rapidly ionizes to He II or remains in the He I configuration.

On Figure 2 are shown the contributions of the lines of He I to the total radiative acceleration of He. They were obtained with four different treatments of momentum transfer in He I. The simplest approximation assumes that there is only one diffusion coefficient for He, which is given by a simple average of the diffusion coefficients of the different states of ionization (*dotted line*). There is, in this treatment, no amplification of the effect of He I line photons by the large diffusion coefficient of He I.

The second approximation assumes that, after a photon is absorbed by a line of He I, the momentum is entirely used by He I (*dashed line*) with the large diffusion coefficient of He I. It is implicitly assumed that all states of ionization are separate.

The third approximation assumes that, after absorption, the atom goes back rapidly to the ground state of He I and travels with the large diffusion coefficient of He I but only until it photoionizes from the ground state (*dash-dotted line*). States of ionization are coupled through photoionization and radiative recombination only. As can be seen, the radiative acceleration is greatly reduced.

The fourth case (*solid line*) takes into account the fact that, after absorption, there is a probability for the electron in the upper state to ionize by collision instead of returning to the ground state. This can be described by a random walk (Michaud *et al.* 1979). The probability of returning to the ground state and of, later, photoionizing as in the third approximation, is also included. This case takes into account all possible processes and corresponds to that identified by He I_L in Figure 1*a*.

A comparison of the different curves shows that the large amplification of the radiative acceleration by the large diffusion coefficient of He I is nearly completely eliminated as soon as the photoionization from the ground state is included (*dash-dotted line*). Adding collisional ionization (*solid line*) hardly changes the result. Furthermore, the simplest approximation (*dotted line*) gives essentially the same result as the most complete calculation (*solid line*). This is simply understood. Rapid ionization from the ground state prevents any amplification of the radiative acceleration transmitted through the lines of He I. This rapid ionization can be traced to the high T_{eff} of the stars studied here. Where the contribution of the lines of He I is maximum, the radiation temperature is already large enough that photoionization is much more rapid than deviation by collisions for He I, reducing considerably the efficiency of the radiation transmitted through the lines of He I (see eq. [6.11*a*] of Montmerle and Michaud 1976). It should be noted that at $T_{\mathrm{eff}} = 40{,}000$ K, in the higher gravity model (not shown), the lines of He I contribute more than those of He II to the radiative acceleration in the line-forming region. This is caused both by the smaller ionization of He I and by the larger collision frequency at higher gravity: the relative importance of collisions to photoionizations increases as gravity increases and a larger fraction of the momentum is spent by He I before it is ionized. One should not conclude that collisions are never important in radiative acceleration calculations. They are negligible here because the radiation temperature is high, and hence photoionization dominates.

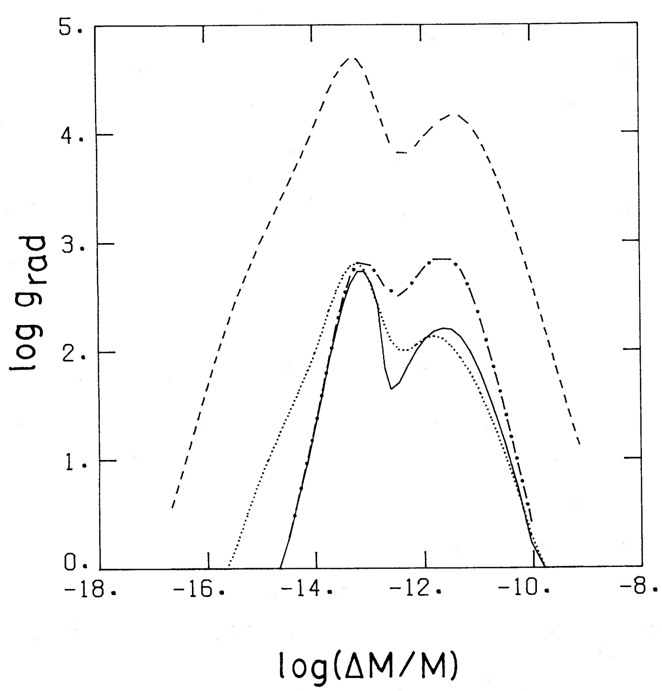

FIG. 2.—Contribution of the lines of He I to the radiative acceleration in the model at $T_{\mathrm{eff}} = 40{,}000$ K, $\log g = 5.0$, $N(\mathrm{He})/N(\mathrm{H}) = 0.03$. The solid line is the same as that identified by He I_L on Fig. 1*a*. The different lines correspond to different approximations for the momentum transfer within the atom. They are discussed in detail in § IIIc.

d) Other Approaches to g_R

Figure 3 shows a comparison of radiative accelerations calculated with different approximations (same parameters as in Fig. 1*a*). The results of the non–LTE calculations are represented by the dashed line, and they serve as a reference to evaluate the effect of various approximations. The LTE (*dash-dotted line*) and approximate non–LTE (*solid-line*) calculations described in § II*c* are displayed, together with the results obtained using the fit (*dotted line*) of Michaud *et al.* (1979). Not surprisingly this is the poorest of the approximations; however it differs at most by a factor of 3 from the non–LTE results. There are applications for which such an accuracy is sufficient. One should not generalize this result, however: larger errors could result from applying to atmospheres a formula derived for stellar interiors. Both the LTE and approximate non–LTE treatments are better approximations. In particular the latter is

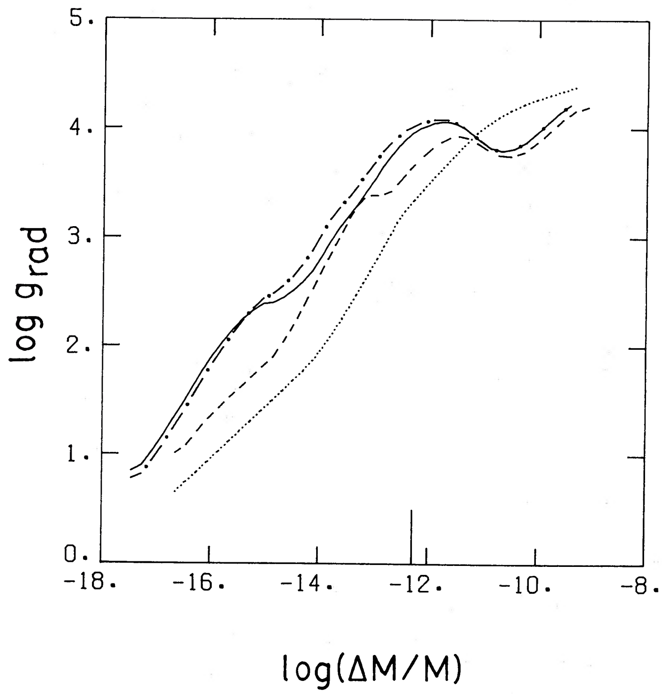

FIG. 3.—Total radiative acceleration on He as a function of the mass above the point of interest calculated with different approximations. The dashed line corresponds to the full non–LTE calculation. The dash-dotted and solid lines represent the LTE and approximate non–LTE calculations, respectively. The dotted line corresponds to the fit of Michaud *et al.* (1979).

close to the non–LTE results throughout the line-forming region, which suggests that it includes the dominant non–LTE effect in this case.

e) Uncertainties in the Model Atmospheres

Recently, more sophisticated non–LTE model atmospheres have become available (Anderson 1985; Werner 1986), which include more detailed model atoms for hydrogen and helium in the calculations and even allow non–LTE metal line blanketing to be treated. We have calculated radiative accelerations from such non–LTE model atmospheres (provided by K. Werner) which include hydrogen and helium line blanketing (72 line transitions) self-consistently (for details, see Heber, Werner, and Drilling 1988). No metal ions were included. In the outer regions of these models ($\tau_{5000} \leq 0.01$), the radiative acceleration of He is larger than in the models used in this paper by a factor of about 10. In the line-forming region, however, the difference is relatively small. The large increase can be traced to an increase of the flux in the He II continuum, which is related to an increase of the He III population. The coupling of the H and He lines to the model provides additional heating of the outer layers of the star. This might be unrealistic because important cooling agents (e.g., resonance lines of C IV) are neglected. Anderson (1985) has calculated a single non–LTE model at $T_{\rm eff} = 35{,}000$ K, log $g = 4.0$ with carbon lines and found that the outer layers are cooled down to the LTE level. Therefore, radiative accelerations for the outermost regions (above the line-forming region) remain uncertain until non–LTE model atmospheres with full metal line blanketing become available. In the line-forming regions, however, our results are affected only marginally by the model uncertainties.

IV. DISCUSSION

Clearly, a cosmological He abundance [N(He)/N(H) = 0.1] is *not* supported by radiative acceleration in the line-forming region in any of the models considered. This result has implications for at least two problems. First, radiative support of He cannot be the cause of the appearance of the He-rich sdO stars ($T_{\rm eff} > 40{,}000$ K; Hunger *et al.* 1981). Radiative acceleration, being always much smaller than gravity for normal He abundances, cannot lead to He overabundances. Indeed even for an abundance of N(He)/N(H) = 0.01, the radiative acceleration is about 10 times smaller than gravity in the line-forming region at all $T_{\rm eff}$ and log g considered. The radiative accelerations calculated here are expected to be much more accurate than a factor of 10 (in the line-forming regions) so that it is well established that radiative acceleration cannot support He against gravity in these objects. Second, diffusion is expected to lead to underabundances of He in all sdOB stars, in agreement with observations. The expected underabundances are larger than observed since using the observed He abundance in the best possible model for Feige 110 leads to a radiative acceleration 10 times smaller than needed to stop gravitational settling. Using the diffusion coefficients of Paquette *et al.* (1986), the diffusion time scale of He II, at an optical depth of $\tau_{5000} = 1$, is calculated to be about 10^3 yr in Feige 110. Other phenomena must be involved to keep the He abundance from decreasing more than observed.

The nature of the dominant competing mechanism is still uncertain. Meridional circulation and turbulence induced by differential rotation have not been ruled out though they would require large rotational velocities. In the case of Feige 110 the observed projected rotational velocity is small: $v \sin i < 20$ km s^{-1} (Heber 1989). The effect of meridional circulation has been shown to decrease rapidly as gravity is increased (Michaud 1982). Mass loss is a definite possibility. It has already been shown to be important to model the Si underabundance in similar objects: a mass-loss rate of about $2 \times 10^{-15}\ M_{\odot}$ yr^{-1} has been shown (Michaud *et al.* 1985) to account for the observed large underabundances of Si in sdOB stars. Detailed models involving separation in the atmosphere and envelope are needed to determine the expected He abundance. For the smaller He abundances, radiative acceleration may play a role below the atmosphere since its importance is comparable to that of gravity at a mass fraction of $\Delta M/M = 10^{-10}$. Such calculations are outside the scope of this paper.

A comparison of radiative accelerations obtained with various approximations is useful to determine the degree of sophistication needed in future work on He. It should first be noted that the radiative accelerations obtained with approximations appropriate to stellar interiors cannot generally be trusted in stellar atmospheres. For He, the fit of Michaud *et al.* (1979) is, here, within a factor of 3 of the non–LTE results, which may be sufficient for certain purposes. Furthermore the LTE and approximate non–LTE treatments give acceptable results with much less effort than complete non–LTE calculations. In particular the approximate non–LTE calculation described here can be obtained easily from LTE models, and gives satisfactory results throughout the line-forming region and the whole region where radiative acceleration can play a role. However, this reasonable agreement is shown here only for the He atom. One should not conclude too rapidly that the LTE calculations are always a good approximation. Results are presented elsewhere (Bergeron *et al.* 1988) which show that the LTE and non–LTE radiative acceleration of Si differ by orders of magnitude in hydrogen-rich subdwarf stars.

We would like to stress the importance of further work on stellar atmosphere models. It was described in § III*e* how a different set of model atmospheres can increase the radiative acceleration in the outer atmosphere by a factor of up to 10. This situation is clearly unsatisfactory and improved model atmospheres are needed. However, even the large change in the outer temperature obtained with these atmospheres does not change our main result that diffusion leads to He underabundances, but that the He abundance should be smaller than observed in the sdB and sdOB stars and that diffusion cannot explain the He-rich sdO stars.

Finally these calculations could be significantly improved by a better determination of the momentum transfer after photoionization (see § II*b*). Since the largest contribution to radiative acceleration comes from photoionization (labeled He II_C and He III_C on Fig. 1) over part of the envelope, it is important that the efficiency of this process be better determined. Calculations of how the photon momentum is shared between the electron and the ion for excited states of hydrogenoid ions and for the ground and excited states of He I are possible now and should be carried out.

We thank S. Vennes for his initial contribution to some of these calculations and K. Werner for providing us with unpublished model atmospheres. This work was supported in part by NSERC Canada. Computing funds were kindly provided by the Centre de Calcul of the Université de Montréal.

REFERENCES

Anderson, L. S. 1985, *Ap. J.*, **298**, 848.
Baschek, B., Höflich, P., and Scholz, M. 1982, *Astr. Ap.*, **112**, 76.
Baschek, B., Kudritzki, R. P., Scholz, M., and Simon, K. P. 1982, *Astr. Ap.*, **108**, 387.
Baschek, B., and Norris, J. 1975, *Ap. J.*, **199**, 694.
Bassalo, J. M., Cattani, M., and Walder, V. S. 1982, *J. Quant. Spectrosc. Rad. Transf.*, **28**, 75.
Bergeron, P., Wesemael, F., Michaud, G., and Fontaine, G. 1988, *Ap. J.*, **332**, 964.
Chapman, S., and Cowling, T. G. 1970, *The Mathematical Theory of Non-uniform Gases* (3d ed.; Cambridge: Cambridge University Press).
Dimitrijevic, M. S., and Sahal-Bréchot, S. 1984, *Astr. Ap.*, **136**, 289.
Greenstein, J. L., and Sargent, A. I. 1974, *Ap. J. Suppl.*, **28**, 157.
Griem, H. R. 1960, *Ap. J.*, **132**, 883.
Groth, H. G., Kudritzki, R. P., and Herber, U. 1985, *Astr. Ap.*, **152**, 107.
Heber, U. 1986, *Astr. Ap.*, **155**, 33.
———. 1989, in preparation.
Heber, U., Hamann, W.-R., Hunger, K., Kudritzki, R. P., Simon, K. P., and Méndez, R. H. 1984*a*, *Astr. Ap.*, **136**, 331.
Heber, U., Hunger, K., Jonas, G., and Kudritzki, R. P. 1984*b*, *Astr. Ap.*, **130**, 119.
Heber, U., Werner, K., and Drilling, J. S. 1988, *Astr. Ap.*, **194**, 223.
Hunger, K., Gruschinske, J., Kudritzki, R. P., and Simon, K. P. 1981, *Astr. Ap.*, **95**, 244.
Kudritzki, R. P., Simon, K. P., Lynas-Gray, A. E., Kilkenny, D., and Hill, P. W. 1982, *Astr. Ap.*, **106**, 254.
Kurucz, R. L. 1970, *Smithsonian Astrophysical Observatory Spec. Rept.* 309.
Lamontagne, R., Wesemael, F., and Fontaine, G. 1987, *Ap. J.*, **318**, 844.
Lamontagne, R., Wesemael, F., Fontaine, G., and Sion, E. M. 1985, *Ap. J.*, **299**, 496.
Lynas-Gray, A. E., Heber, U., Kudritzki, R. P., and Simon, K. P. 1984, in *Proc. 4th European IUE Conf.* (ESA SP-218), p. 285.
Martel, A. 1979, Internal Rept., Université de Montréal.
Michaud, G. 1970, *Ap. J.*, **160**, 641.
———. 1982, *Ap. J.*, **258**, 349.
———. 1987, *Phys. Scripta*, **36**, 112.
Michaud, G., Bergeron, P., Wesemael, F., and Fontaine, G. 1985, *Ap. J.*, **299**, 741.
Michaud, G., Charland, Y., Vauclair, S., and Vauclair, G. 1976, *Ap. J.*, **210**, 447.
Michaud, G., Montmerle, T., Cox, A. N., Magee N. H., Hodson, S. W., and Martel, A. 1979, *Ap. J.*, **234**, 206.
Mihalas, D. 1978, *Stellar Atmospheres* (2d ed.; San Francisco: Freeman).
Montmerle, T., and Michaud, G. 1976, *Ap. J. Suppl.*, **31**, 489.
Paquette, C., Pelletier, C., Fontaine, G., and Michaud, G. 1986, *Ap. J. Suppl.*, **61**, 177.
Sommerfeld, A. 1939, *Atombau und Spectrallinien*, Vol. **2**, (5th ed.; Braunschweig: Vieweg & Sohn).
Vennes, S. 1985, Internal Rept., Université de Montréal.
Werner, K. 1986, *Astr. Ap.*, **161**, 183.
Wesemael, F. 1981, *Ap. J. Suppl.*, **45**, 177.
Wesemael, F., Auer, L. H., Van Horn, H. M., and Savedoff, M. P. 1980, *Ap. J. Suppl.*, **43**, 159.
Wiese, W. L., Smith, M. W., and Glenon, B. M. 1966, *Atomic Transition Probabilities*, Vol. **1** (NSRDS-NBS 4) (Washington: US Government Printing Office).

P. Bergeron, G. Michaud, and F. Wesemael: Département de Physique, Université de Montréal, Montréal H3C 3J7, Canada

U. Heber: Institut für Theoretische Physik und Sternwarte der Universität Kiel, Olshausenstrasse 40, D-2300 Kiel 1, Federal Republic of Germany